Counting Statistics of Single Electron Transport in a Semiconductor Quantum Dot

S. Gustavsson[1], R. Leturcq[1], B. Simovič[1], R. Schleser[1], T. Ihn[1], P. Studerus[1], K. Ensslin[1], D. C. Driscoll[2], and A. C. Gossard[2]

[1] Solid State Physics Laboratory, ETH Zürich, 8093 Zürich, Switzerland

[2] Materials Departement, University of California, 93106 Santa Barbara, USA

Abstract. By using a quantum point contact as a charge detector, we show the measurement of current fluctuations in a semiconductor quantum dot by counting electrons tunneling through the system one by one. This method gives direct access to the full counting statistics of current fluctuations. In the sequential tunneling regime, we show the suppression of the noise compared to its classical Poissonian value, which is expected due to Coulomb blockade.

1 Introduction

In addition to the mean of the current, current fluctuations are very important in order to understand the transport mechanisms in a conductor [1]. In particular, they provide information on the involved charge. Many experiments have been concerned with measuring the shot noise, which is the variance of the current fluctuations. Not only the variance can be of interest, but also higher moments of current fluctuations could provide new information on the system, as it is widely used in quantum optics for probing photon entanglement [2]. For electronic systems, the third moment is of particular interest since it is not affected by the thermal noise, and could be used to determine the nature of the charge transport at high temperature [3, 4].

For independent particles, current fluctuations are expected to follow a Poissonian distribution. In the case of a quantum dot (QD) in the sequential tunneling regime, the noise is suppressed compared to the Poissonian distribution due to correlations between the electrons tunneling through the QD [5]: because of Coulomb blockade, an electron occupying the QD blocks the transport of the next electron. This suppression is maximum when the QD is symmetrically coupled to the leads, but vanishes for asymmetrically coupled QDs since the transport is limited by the weakly coupled contact. Few experiments on vertical quantum dots could measure a suppression of the noise [6–8], but measurements on lateral quantum dots are difficult due the very low current level involved.

An alternative way of measuring current fluctuations is to detect directly the charges traveling through a conductor. This method has been suggested

R. Haug (Ed.): Advances in Solid State Physics,
Adv. in Solid State Phys. **46**, 31–43 (2008)

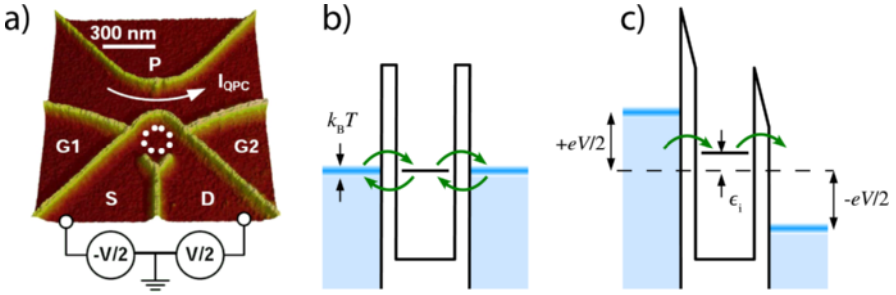

Fig. 1. (**a**) AFM micrograph of the oxide lines defining the nanostructure. The QD (*circle*) is connected to two leads S and D, and a nearby QPC is electrostatically coupled to the QD. Voltages applied on the lateral gates G1, G2 and P allow to tune respectively the coupling to source (S) and drain (D), and the conductance through the QPC. A bias voltage V is applied between S and D, and the conductance through the QPC is measured by applying a constant dc voltage and measuring the current I_{QPC}. (**b**) Energy diagram of the QD connected to the leads in the case where the level in the QD is aligned with the chemical potential in the leads, leading to equilibrium charge fluctuations in the QD. (**c**) Energy diagram of the QD in the case $eV/2 - \epsilon_i \gg k_{\mathrm{B}}T$, for which electrons tunnel into the QD from the source and tunnel out of the dot through the drain

by theories known as full counting statistics [9], and has been used since then as a theoretical tool to calculate current fluctuations in conductors. However, first attempts to measure the current by counting electrons could not achieve enough resolution in order to study the statistics of current fluctuations [10–12]. By using a quantum point contact (QPC) as a charge detector, we show here the direct measurement of the full distribution of current fluctuations in a semiconductor quantum dot [13].

2 Experimental Methods

The sample shown in Fig. 1a has been realized by local oxidation of the surface of a GaAs/AlGaAs heterostructure using an atomic force microscope. The oxide line obtained by scanning the biased AFM tip on top of the surface depletes the two-dimensional electron gas situated 34 nm below the surface, and allows to create high quality nanostructures [14, 15]. Our sample consists in a quantum dot (QD) connected to two leads, source (S) and drain (D), and a nearby quantum point contact (QPC) capacitively coupled to the QD. The lateral gates G1 and G2 are used to tune the coupling of the QD to the leads, while the gate P controls the conductance of the QPC. The measurements have been done in a ^{3}He/^{4}He dilution refrigerator. The electronic temperature, measured by the Coulomb peak width, is 230 mK.

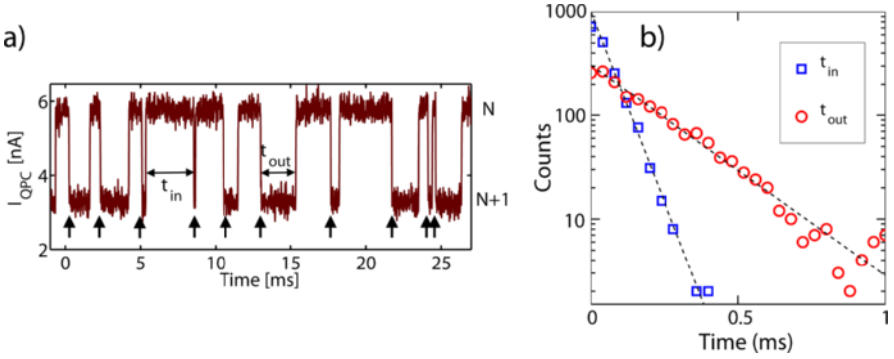

Fig. 2. (**a**) Typical time trace of the current measured through the QPC for a constant bias voltage applied on the QPC. The two levels correspond to zero (N) and one ($N+1$) excess electron in the QD. $\tau_{\rm in}$ is the time it takes for an electron to tunnel into the QD, and $\tau_{\rm out}$ the time it takes for an electron to tunnel out of the QD. (**b**) Probability density of the times $\tau_{\rm in}$ and $\tau_{\rm out}$. The *points* are experimental data, and the *lines* are fits with (13)

The strong dependence of the conductance of a QPC on the neighboring electrostatic potential makes it a very sensitive electrometer. A QPC can detect the charge state of a QD [16]. Time resolved detection of single electrons tunneling in and out of a QD has been used to detect spin states in a single [17] and double quantum dots [18], and to measure equilibrium charge fluctuations in a QD connected to a single lead [19, 20]. In these last experiments, the configuration was similar to the one depicted in Fig. 1b, in which thermal fluctuations induce hopping of electrons back and forth from one contact to the same contact (the second contact being pinched-off in these experiments). Here we propose to use the QPC to detect charge fluctuations in a QD connected symmetrically to two leads S and D. For a sufficiently large bias voltage applied between the two leads, the only possibility for an electron to tunnel through the QD is to come from the source contact, and to leave by the drain contact (see Fig. 1c). In this regime, the charge fluctuations measured in the QD are directly related to the fluctuations of the current through the QD, measured by detecting the tunneling of single electrons.

A typical time trace of the current measured through the QPC is shown in Fig. 2a. Fluctuations of charges in the QD are monitored by this current, which fluctuates between two states, corresponding to zero (upper states, N) and one (bottom state, $N+1$) excess electron in the QD. The trace of Fig. 2a shows the high signal-to-noise ratio in this set-up, allowing to measure single tunneling events with a short time resolution.

For a large bias voltage applied between S and D on the QD, a pair of one step downwards and one step upwards corresponds to one electron tunneling though the QD. The current through the QD can then be deduced from

time traces similar to the one of Fig. 2a by counting the number of electron tunneling into the QD (corresponding to a step $N \rightarrow N+1$, see arrows in Fig. 2a, given that, due to Coulomb blockade, only one electron can enter the QD at a time. The same analysis on electrons tunneling out of the QD gives the same result. The current is simply given by the number of electrons tunneling through the QD in a given time interval. The bandwidth of the QPC circuit is 30 kHz, determined by the capacitance of the cables and the feedback resistor of the I–V converter. This bandwidth limits the current we can measure by counting electrons to 5 fA, while the lower limit is determined by the length of the time trace we take.

This way of counting electrons passing through a conductor to measure the current has been achieved in different configurations only very recently [10–12]. However, while these experiments were limited to measurement of the mean current, our measurement shows that we can measure not only the mean current, but also its fluctuations in time. In particular, we can deduce the current noise, which has been widely used to characterize mesoscopic systems [1]. But we can go even further, and measure the full distribution function of the current fluctuations.

3 Counting Statistics in the Sequential Tunneling Regime

The full counting statistics has been calculated for a QD in the sequential tunneling regime, and in this section we summarize the main results of [21] adapted to our way of counting events. The evolution of the occupancy of the QD, with 0 or 1 excess electron, can be describe by the rate equation:

$$\frac{\mathrm{d}}{\mathrm{d}t}\begin{pmatrix}0\\1\end{pmatrix} = \begin{pmatrix}-\Gamma_{\mathrm{in}} & \Gamma_{\mathrm{out}}\\ \Gamma_{\mathrm{in}} & -\Gamma_{\mathrm{out}}\end{pmatrix}\begin{pmatrix}0\\1\end{pmatrix} , \tag{1}$$

with

$$\Gamma_{\mathrm{in}} = g_{\mathrm{s}}\Gamma_{\mathrm{L}} f_{\mathrm{L}}(\epsilon_i) + g_{\mathrm{s}}\Gamma_{\mathrm{L}} f_{\mathrm{L}}(\epsilon_i) \tag{2}$$

$$\text{and} \quad \Gamma_{\mathrm{out}} = \Gamma_{\mathrm{L}}\left(1 - f_{\mathrm{L}}(\epsilon_i)\right) + \Gamma_{\mathrm{R}}\left(1 - f_{\mathrm{R}}(\epsilon_i)\right) , \tag{3}$$

where f_{L} and f_{R} are the Fermi distributions in the left and right leads, ϵ_i is the energy of the level in the quantum dot, and g_{s} is the spin degeneracy of this level. These rates can be simplified in the case of large bias voltage, $|\pm eV/2 - \epsilon_i| \gg k_{\mathrm{B}}T$, for which the electron tunnels into the QD only through a single lead, the source (being either left or right lead, depending on the sign of the bias voltage), and tunnels out of the QD through the other contact, the drain:

$$\Gamma_{\mathrm{in}} = g_{\mathrm{s}}\Gamma_{\mathrm{L(R)}} = \Gamma_{\mathrm{s}} \qquad \text{and} \qquad \Gamma_{\mathrm{out}} = \Gamma_{\mathrm{R(L)}} = \Gamma_{\mathrm{D}} . \tag{4}$$

Here, $\Gamma_{\rm s}$ and $\Gamma_{\rm D}$ are effective tunneling rates which take into account possible spin degeneracy. $\Gamma_{\rm s}$ and $\Gamma_{\rm D}$ are assumed to be energy independent. In this limit, the model can be extended to the transport through multiple levels in the QD, the effective tunneling rates being the sum of the tunneling rates through individual levels.

To perform the counting statistics, we need to introduce a counting field $e^{i\chi}$ in the rate equation. In our case, we count electrons tunneling into the QD, and the matrix can be written:

$$M(\chi) = \begin{pmatrix} -\Gamma_{\rm in} & \Gamma_{\rm out} \\ \Gamma_{\rm in} e^{i\chi} & -\Gamma_{\rm out} \end{pmatrix} . \tag{5}$$

The distribution function of the number n of electrons tunneling through the quantum dot during a time t_0 can be calculated with the cumulant-generating function $S(\chi)$:

$$P(n) = \int_{-\pi}^{\pi} \frac{{\rm d}\chi}{2\pi} e^{-S(\chi)-n\chi} , \tag{6}$$

where $S(\chi)$ is given by the lowest eigenvalue of $M(\chi)$, $\lambda_0(\chi)$:

$$S(\chi) = -\lambda_0(\chi) t_0 = \frac{t_0}{2}\left[\Gamma_{\rm s} + \Gamma_{\rm D} - \sqrt{(\Gamma_{\rm s}-\Gamma_{\rm D})^2 + 4\Gamma_{\rm s}\Gamma_{\rm D} e^{-i\chi}}\right] . \tag{7}$$

From the distribution function $P(n)$, one can calculate all central moments characterizing the current fluctuations. The three first central moments μ_i, in which we are interested in the following, coincide with the cumulants C_i. They can then be deduced from the cumulant-generating function. The mean current is given by the mean, or the first cumulant C_1, of the distribution:

$$I = \frac{ie}{t_0} C_1 = \frac{ie}{t_0}\left(\frac{{\rm d}S}{{\rm d}\chi}\right)_{\chi=0} = -e\frac{\Gamma_{\rm s}\Gamma_{\rm D}}{\Gamma_{\rm s}+\Gamma_{\rm D}} . \tag{8}$$

The symmetrized shot noise is given by the variance, or the second cumulant C_2, of the distribution:

$$S_I = \frac{2e^2}{t_0} C_2 = \frac{2e^2}{t_0}\left(\frac{d^2 S}{d\chi^2}\right)_{\chi=0} , \tag{9}$$

... from which we can calculate the Fano factor:

$$F_2 = \frac{S_I}{2eI} = \frac{C_2}{iC_1} = \frac{\Gamma_{\rm s}^2 + \Gamma_{\rm D}^2}{(\Gamma_{\rm s}+\Gamma_{\rm D})^2} = \frac{1}{2}\left(1 + a^2\right) , \tag{10}$$

where $a = (\Gamma_{\rm s} - \Gamma_{\rm D})/(\Gamma_{\rm s} + \Gamma_{\rm D})$ is the asymmetry of the coupling. This result recovers the earlier calculations for the shot noise in a quantum dot [5], and shows the reduction of the noise by a factor 1/2 for a QD symmetrically

coupled to the leads, while the Poissonian limit, $F_2 = 1$, is reached for an asymmetrically coupled QD.

Finally we are also interested in the third central moment, or third cumulant C_3, of the fluctuations, which characterizes the asymmetry of the distribution (skewness):

$$S_I^3 = \frac{ie^3}{t_0} C_3 = \frac{ie^3}{t_0} \left(\frac{d^3 S}{d\chi^3} \right)_{\chi=0} , \tag{11}$$

which can also be characterized by its normalized value:

$$F_3 = \frac{C_3}{C_1} = \frac{\Gamma_\mathrm{s}^4 - 2\Gamma_\mathrm{s}^3\Gamma_\mathrm{D} + 6\Gamma_\mathrm{s}^2\Gamma_\mathrm{D}^2 - 2\Gamma_\mathrm{s}\Gamma_\mathrm{D}^3 + \Gamma_\mathrm{D}^4}{(\Gamma_\mathrm{s} + \Gamma_\mathrm{D})^4} = \frac{1}{4}\left(1 + 3a^4\right) . \tag{12}$$

This results shows the strong reduction of the third moment, by a factor 1/4, for a symmetrically coupled QD, and the Poissonian limit, $F_3 = 1$, for an asymmetrically coupled quantum dot.

4 Determination of the Individual Tunneling Rates

In order to make a quantitative comparison of the experimental results with the theory, it is important to determine the tunneling rates Γ_s and Γ_D, which are the only parameters of our model. In the time trace of Fig. 2a, the time τ_in represents the time an electron needs to tunnel into the QD, while the time τ_out is the time an electron needs to tunnel out of the QD. In the case where tunneling events are uncorrelated, the probability densities are expected to follow exponential functions:

$$P_{\tau_\mathrm{in}} \propto \Gamma_\mathrm{in} \exp(-\Gamma_\mathrm{in}\tau_\mathrm{in}) \qquad \text{and} \qquad P_{\tau_\mathrm{out}} \propto \Gamma_\mathrm{out} \exp(-\Gamma_\mathrm{out}\tau_\mathrm{out}) . \tag{13}$$

Figure 2b shows that these relations are well followed experimentally, proving that the tunneling events are uncorrelated. The tunneling rates Γ_in and Γ_out can be determined either by fitting the data in Fig. 2b with (13), or by taking the averages $\Gamma_\mathrm{in} = 1/\langle\tau_\mathrm{in}\rangle$ and $\Gamma_\mathrm{out} = 1/\langle\tau_\mathrm{out}\rangle$.

At large bias voltage, $|\pm eV/2 - \epsilon_i| \gg k_\mathrm{B}T$, the only possibility for an electron to tunnel in is to come from the source contact, and the only possibility to tunnel out is to go to the drain contact (see Fig. 1c). In this case, the tunneling rates from source and to drain can be directly calculated from the tunneling times considering that $\Gamma_\mathrm{s} = \Gamma_\mathrm{in}$ and $\Gamma_\mathrm{D} = \Gamma_\mathrm{out}$. As we emphasized in the previous section, this model can be extended to several levels.

5 Distribution Function of Current Fluctuations

In order to determine the distribution function of current fluctuations from the measurement, a time trace of length $T = 0.5\,\mathrm{s}$ is divided into intervalles

of length t_0, during which we count the number n of electrons tunneling into the QD. The distribution function of the number of events in this time intervalle t_0 is shown in Fig. 3a, and characterizes directly the current fluctuations. In order to compare the experimental result with the theory presented in Sect. 3, the tunneling rates are first determined as explained in Sect. 4, and then included in (7) and (6) in order to determine the probability distribution $P_{t_0}(n)$. The result is shown as a plain line in Fig. 3a. The agreement with the experimental data is striking, knowing that no adjustable parameters are used.

From the time traces, we can also calculate the central moments given by $\mu = \langle n \rangle$ and $\mu_i = \langle n^i - \langle n \rangle^i \rangle$. For $i \leq 3$, the central moments are equal to the cumulants. For this reason we will use the same notation C_i for both, but experimentally only the central moments are calculated.

An important parameter for the analysis is the time t_0 in which we count the events. In Fig. 3b we show the values of the second and third central moments determined for several values of t_0. For small time $t_0 \ll 1/\Gamma_\mathrm{s}, 1/\Gamma_\mathrm{D}$, we expect to measure either 0 or 1 event, meaning that the resulting distribution will tend to a Bernoulli distribution, with a probability of measuring one event being:

$$p = \frac{\langle n_\mathrm{total} \rangle t_0}{T} = t_0 \frac{\Gamma_\mathrm{s}\Gamma_\mathrm{D}}{\Gamma_\mathrm{s} + \Gamma_\mathrm{D}} \ . \tag{14}$$

$\langle n_\mathrm{total} \rangle$ is the average total number of events expected within the time T. The central moments of this Bernoulli distribution are:

$$C_1 = p \quad , \quad C_2 = p(1-p) \quad \text{and} \quad C_3 = p(1-p)(1-2p) \, . \tag{15}$$

Since p tends to 0 when t_0 tends to zero, the normalized central moments $C_2/C_1 = (1-p)$ and $C_3/C_1 = (1-p)(1-2p)$ both tend to 1 when t_0 tends to zero in Fig. 3b. For this reason it is important to choose a time $t_0 > 1/\Gamma_\mathrm{s}, 1/\Gamma_\mathrm{D}$, corresponding to an average number of events measured during t_0 larger than one, $\langle n \rangle > 1$. For all analysis, $\langle n \rangle$ is kept close to 3.

6 Coulomb Diamonds Measured by Counting Electrons

By changing the gate voltage V_G1 and the bias voltage V, we can map out the charge stability diagram of the QD (so called Coulomb diamonds). We have measured the distribution function for each point (V,V_G1), and the three first central moments are shown in Fig. 4. We point out that our method gives the current through the QD only under the condition $| \pm eV/2 - \epsilon_i | \gg k_\mathrm{B}T$, i.e., far from the conduction edges of the Coulomb diamonds. In particular, the enhancement of C_1 along the edges of the Coulomb diamonds is due to equilibrium fluctuation of charges between the QD and the leads (see Fig. 1b) and is not related to the current.

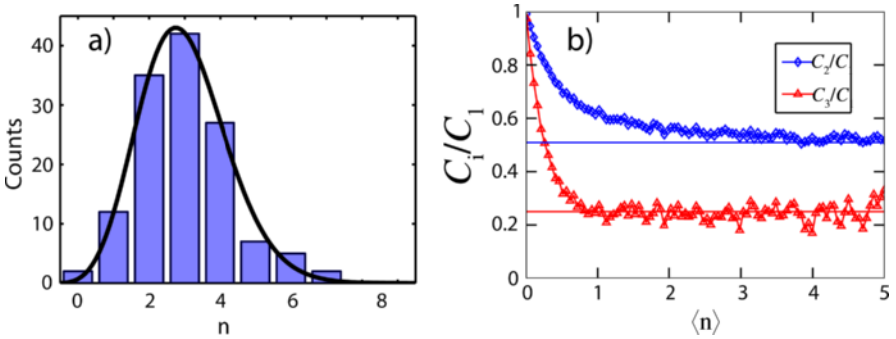

Fig. 3. (**a**) Distribution function of the number of electrons tunneling into the QD during a time t_0, obtained for $V_{G1} = -44\,\mathrm{mV}$ and at large bias voltage. In this configuration, the tunneling rates are $\Gamma_s = 1748\,\mathrm{Hz}$ and $\Gamma_D = 1449\,\mathrm{Hz}$, determined as described in Sect. 4. The *red line* is calculated from (6) with the same tunneling rates. (**b**) Normalized central moments determined for different values of the time t_0, represented in the x-axis by the average number of event measured during the time t_0, $\langle n\rangle = t_0\Gamma_s\Gamma_D/(\Gamma_s + \Gamma_D)$. The *horizontal lines* are the expected values

Figure 4a is very similar to conventional Coulomb diamonds measured by transport in quantum dots, and show well resolved excited states. However, the currents measured here are lower than 1 fA, and are well below what could be achieved with any conventional current measurement. The second central moment shows features that are very similar to the mean, and we have shown that excited states can also be resolved [13, 22], as it has been also observed for noise measurements in QDs formed in carbon nanotubes [23].

In most of the regions, the central moments correspond to a sub-Poissonian noise, with $C_2/C_1 < 1$ and $C_3/C_1 < 1$. This reduction of the noise is characteristic of a quantum dot in the Coulomb blockade regime, and is compatible with the model of sequential tunneling transport through a single level, or through multiple independent levels. This situation is however not true in the region encircled in Figs. 4b and 4c, corresponding to the chemical potential of one lead being aligned with the chemical potential in the dot ($eV/2 = \epsilon_i$). In this region, the noise is clearly super-Poissonian, with $C_2/C_1 > 1$ and $C_3/C_1 > 1$. This situation is of great interest since it corresponds to bunching of electrons, which is not expected for the transport of independent fermions. It is also not expected for interacting electrons in the model of sequential tunneling presented in Sect. 3, which can be extended to the situation where $eV/2 = \epsilon_i$. Using an extended model, we can show that this bunching is due to transport through two states with very different tunneling rates, given that the excited state has a long relaxation time [22].

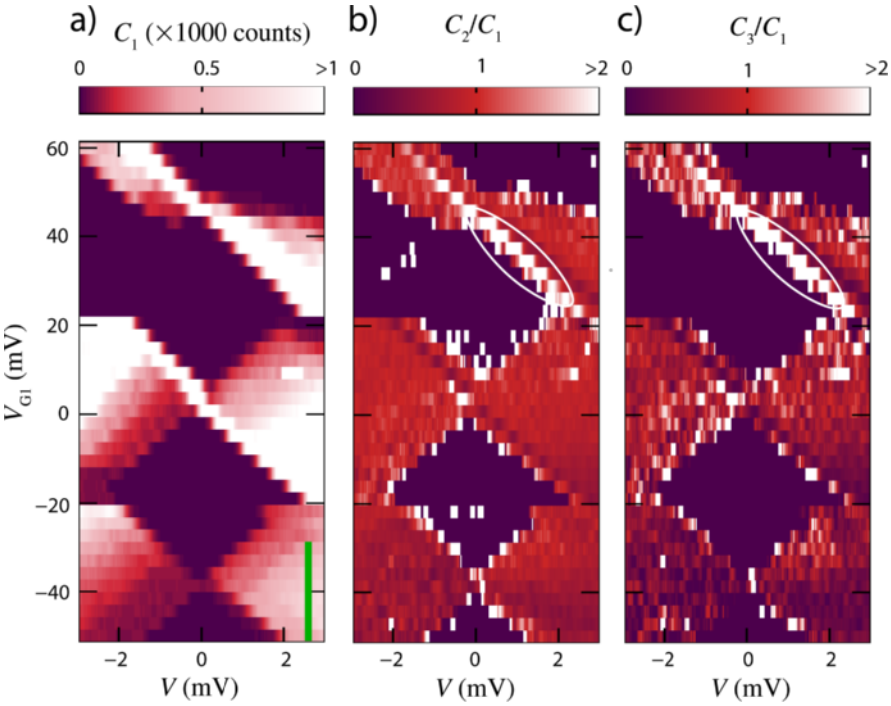

Fig. 4. Measurement of the charge stability diagram of the QD as a function of the voltage on gate G1 (used as plunger gate) and the bias voltage V. (**a**) First central moment, proportional to the mean current; (**b**) normalized second central moment, which is the Fano factor of the shot noise; (**c**) normalized third central moment. The *gray* (*green* online) *vertical bar* in (a) represents the range over which the analysis of Fig. 5 is done

7 Counting Statistics and Sub-Poissonian Noise

Equations (10) and (12) show that the second and third normalized cumulants depend on the tunneling rates only through the asymmetry $a = (\Gamma_s - \Gamma_D)/(\Gamma_s + \Gamma_D)$. To further check how the theory applies to our system, we have measured the distribution function for different values of the asymmetry a. Changing the asymmetry is achieved by changing the voltage on the gate G1: in addition to acting as a plunger gate and changing the number of electrons in the QD, as shown in Fig. 4, this gate also modifies the coupling of the source lead. This is shown in particular following the gray (green online) vertical bar in Fig. 4a, for which the asymmetry changes from -0.5 to 1, as shown in the inset of Fig. 5.

In Fig. 5, the second and third central moments are plotted as a function of V_{G1} and a. To increase the resolution, each data point correspond to an

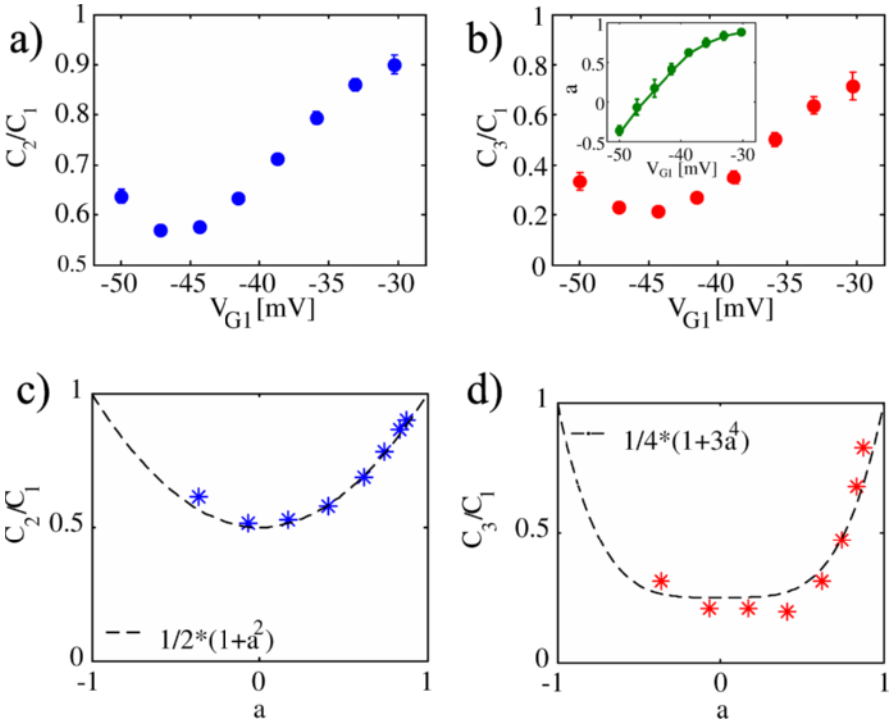

Fig. 5. (**a**,**b**) Second and third normalized central moments as a function of the gate voltage V_{G1}. (**c**,**d**) Same data as a function of the asymmetry of the tunneling rates. The points are experimental data, averaged over several traces in a bias voltage window of $1.5 < V < 3\,\mathrm{mV}$. The lines are the theoretical predictions given by (10) and (12). Inset: asymmetry of the tunneling rates $a = (\Gamma_{\mathrm{s}} - \Gamma_{\mathrm{D}})/(\Gamma_{\mathrm{s}} + \Gamma_{\mathrm{D}})$ vs. the gate voltage V_{G1}

average over 50 time traces at a given gate voltage V_{G1} and in a bias window $1.5 < V < 3\,\mathrm{mV}$, for which a does not change. We have plotted in Figs. 5c and 5d the theoretical predictions for the cumulants given by (10) and (12). Here again, the agreement between experiment and theory is very good, given that there is no adjustable parameter [13].

8 Equilibrium Charge Fluctuations

As pointed out before, the measurement of charge fluctuations in the QD are equivalent to current fluctuations only at large bias voltage, i.e., $|\pm eV/2 - \epsilon_i| \gg k_{\mathrm{B}}T$. This condition is shown in Fig. 6a presenting the central moments as a function of the bias voltage for a fixed gate voltage. While the equivalence between charge and current fluctuations is not valid at small bias

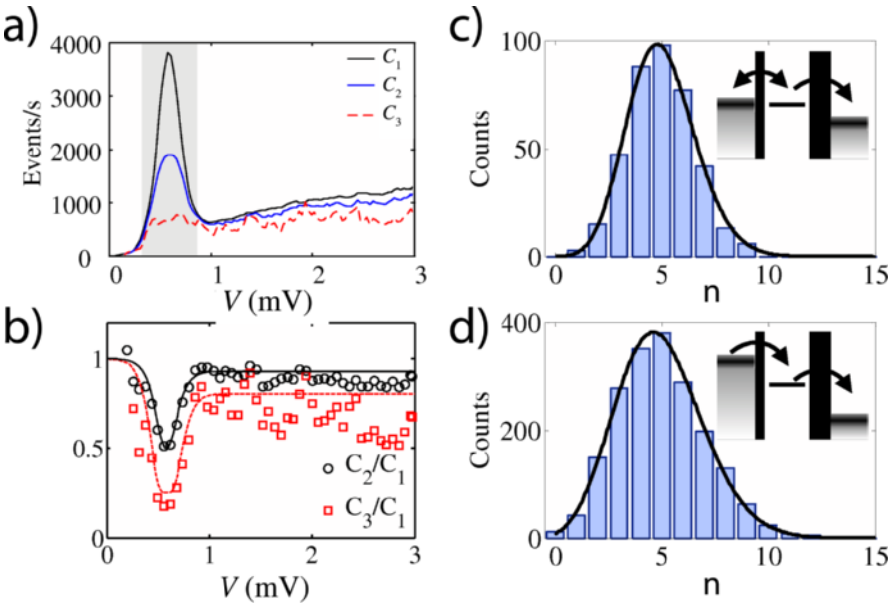

Fig. 6. (**a**) Central moments measured as a function of the bias voltage V for a fixed gate voltage $V_{G1} = -2\,\mathrm{mV}$. The gray region represents the region where the condition $|\pm eV/2 - \epsilon_i| \gg k_B T$ is not valid, and the charge fluctuations in the QD are not directly related to the current fluctuations through the QD. (**b**) Second and third normalized central moments in the same conditions. *Lines* are given by the theory of Sect. 3 extended to take into account equilibrium fluctuations. (**c**) Distribution function of the charge fluctuations at $V = 0.6\,\mathrm{mV}$, corresponding to the scheme in the *inset*. In this case, the chemical potential of the source lead is aligned with the chemical potential of the QD, and the equilibrium fluctuations dominate the charge fluctuations. The effective tunneling rates used for the fit are $\Gamma_{\mathrm{in}} = 7800\,\mathrm{Hz}$ and $\Gamma_{\mathrm{out}} = 7900\,\mathrm{Hz}$. (**d**) Distribution function at large bias voltage, resulting from an averaging of data at large bias voltage $2.5 < V < 3\,\mathrm{mV}$. The effective tunneling rates used for the fit are $\Gamma_{\mathrm{in}} = \Gamma_{\mathrm{s}} = 19500\,\mathrm{Hz}$ and $\Gamma_{\mathrm{out}} = \Gamma_{\mathrm{D}} = 1300\,\mathrm{Hz}$

voltage (gray regions in Fig. 6a), the theory of counting statistics presented in Sect. 3 can still be applied in this case. Taking into account the full expression for the tunneling rates in (2) and (3), including the Fermi distributions in the leads, we can calculate the distribution function of charge fluctuations in the QD (see Fig. 6b).

Qualitatively, the strong reduction of the second and third normalized moments at the conduction edge observed in Fig. 6b can be understood as follows. For $eV/2 \approx \epsilon_i$, the effective tunneling rates are functions of the value of the Fermi distribution at ϵ_i. When increasing the bias voltage, this value changes from 0 to 1, and the effective tunneling rate of the left lead (i.e.,

$\Gamma_{\mathrm{L}} f_{\mathrm{L}}(\epsilon_i)$ in (2)) changes from 0 to Γ_{L}. Considering the tunneling rate of the right lead constant in this region, and with the condition $\Gamma_{\mathrm{R}} \ll \Gamma_{\mathrm{L}}$, the asymmetry of the coupling will then change continuously from -1 to 0 and 1, giving this strong reduction of the normalized central moments to 1/2 and 1/4 when the asymmetry is close to zero. This effect is similar to the suppression of the noise in vertical quantum dots near the conduction edges [6–8].

9 Conclusion

Using a quantum point contact as a charge detector, we have measured the charge fluctuations in a quantum dot at large bias voltage. In this regime, the charge fluctuations are directly related to current fluctuations in the QD. This method allows to measure current and noise levels that could not be reached with conventional current measurements, and is of great interest in order to measure the shot noise in lateral semiconductor quantum dots. In addition to the mean current and the shot noise, this method gives direct access to the distribution function of current fluctuations, known as the full counting statistics.

References

[1] Y. M. Blanter, M. Büttiker, Phys. Rep. **336**, 1–166 (2000)
[2] A. Zeilinger, G. Weihs, T. Jennewein, M. Aspelmeyer, Nature (London) **433**, 230–238 (2005)
[3] B. Reulet, J. Senzier, D. E. Prober, Phys. Rev. Lett. **91**, 196601 (2003)
[4] Y. Bomze, G. Gershon, D. Shovkun, L. S. Levitov, M. Reznikov, Phys. Rev. Lett. **95**, 176601 (2005)
[5] S. Hershfield, J. H. Davies, P. Hyldgaard, C. J. Stanton, J. W. Wilkins, Phys. Rev. B **47**, 1967–1979 (1993)
[6] H. Birk, M. J. M. de Jong, C. Schönenberger, Phys. Rev. Lett. **75**, 1610–1613 (1995)
[7] A. Nauen, I. Hapke-Wurst, F. Hohls, U. Zeitler, R. J. Haug, K. Pierz, Phys. Rev. B **66**, 161303(R) (2002)
[8] A. Nauen, F. Hohls, N. Maire, K. Pierz, R. J. Haug, Phys. Rev. B **70**, 033305 (2004)
[9] L. S. Levitov, H. Lee, G. B. Lesovik, J. Math. Phys. **37**, 4845–4866 (1996)
[10] W. Lu, Z. Ji, L. Pfeiffer, K. W. West, A. J. Rimberg, Nature (London) **423**, 422–425 (2003)
[11] T. Fujisawa, T. Hayashi, Y. Hirayama, H. D. Cheong, Y. H. Jeong, Appl. Phys. Lett. **84**, 2343–2345 (2004)
[12] J. Bylander, T. Duty, P. Delsing, Nature (London) **434**, 361–364 (2005)
[13] S. Gustavsson, R. Leturcq, B. Simovič, R. Schleser, T. Ihn, P. Studerus, K. Ensslin, D. C. Driscoll, A. C. Gossard, Phys. Rev. Lett. **96**, 076605 (2006)
[14] R. Held, S. Lüscher, T. Heinzel, K. Ensslin, W. Wegscheider, Appl. Phys. Lett. **75**, 1134–1136 (1999)

[15] A. Fuhrer, A. Dorn, S. Lüscher, T. Heinzel, K. Ensslin, W. Wegscheider, M. Bichler, Superlattice Microst.. **31**, 19–42 (2002)
[16] M. Field, C. G. Smith, M. Pepper, D. A. Ritchie, J. E. F. Frost, G. A. C. Jones, D. G. Hasko, Phys. Rev. Lett. **70**, 1311–1314 (1993)
[17] J. M. Elzerman, R. Hanson, L. H. Willems van Beveren, B. Witkamp, L. M. K. Vandersypen, L. P. Kouwenhoven, Nature (London) **430**, 431–435 (2004)
[18] J. R. Petta, A. C. Johnson, J. M. Taylor, E. A. Laird, A. Yacoby, M. D. Lukin, C. M. Marcus, M. P. Hanson, A. C. Gossard, Science **309**, 2180–2184 (2005)
[19] R. Schleser, E. Ruh, T. Ihn, K. Ensslin, D. C. Driscoll, A. C. Gossard, Appl. Phys. Lett. **85**, 2005–2007 (2004)
[20] L. M. K. Vandersypen, J. M. Elzerman, R. N. Schouten, L. H. Willems van Beveren, R. Hanson, L. P. Kouwenhoven, Appl. Phys. Lett. **85**, 4394–4396 (2004)
[21] D. A. Bagrets, Y. V. Nazarov, Phys. Rev. B **67**, 085316 (2003)
[22] S. Gustavsson, R. Leturcq, B. Simovič, R. Schleser, T. Ihn, P. Studerus, K. Ensslin, D. C. Driscoll, A. C. Gossard (unpublished)
[23] E. Onac, F. Balestro, B. Trauzettel, C. F. J. Lodewijk, L. P. Kouwenhoven, Phys. Rev. Lett. **96**, 026803 (2006)